Supporting Information for:

Synthesis of poly(stearyl methacrylate)-poly(2-hydroxypropyl methacrylate) diblock copolymer nanoparticles via RAFT dispersion polymerization of 2-hydroxypropyl methacrylate in mineral oil

Csilla György, Saul J. Hunter, Chloé Girou, Matthew J. Derry and Steven P. Armes*

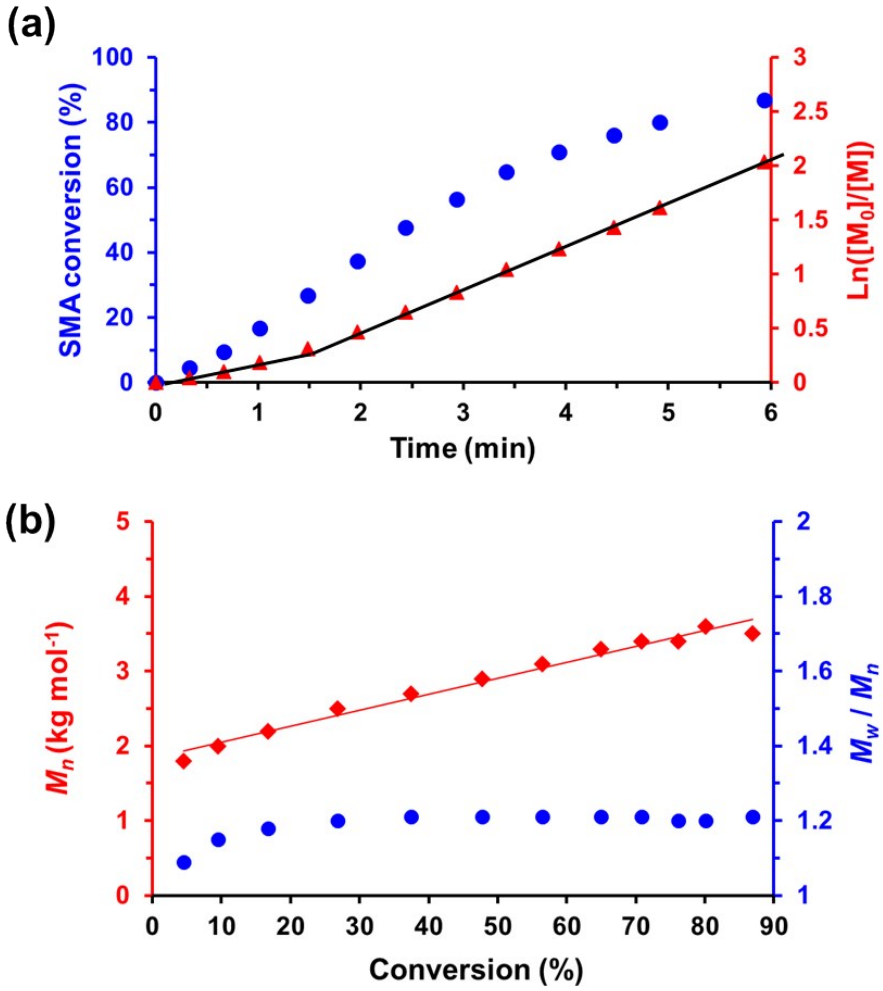

Figure S1. RAFT solution polymerization of SMA in toluene at 50% w/w solids and 70 °C using CPDB as a RAFT agent (target PSMA DP = 5; CPDB/initiator molar ratio = 5.0). **(a)** Conversion *vs*. time (blue circles) and corresponding ln([M]$_0$/[M]) *vs*. time (red triangles) plots. **(b)** Evolution in M_n (red diamonds) and M_w/M_n (blue circles) obtained by THF GPC analysis using a series of near-monodisperse poly(methyl methacrylate) calibration standards.

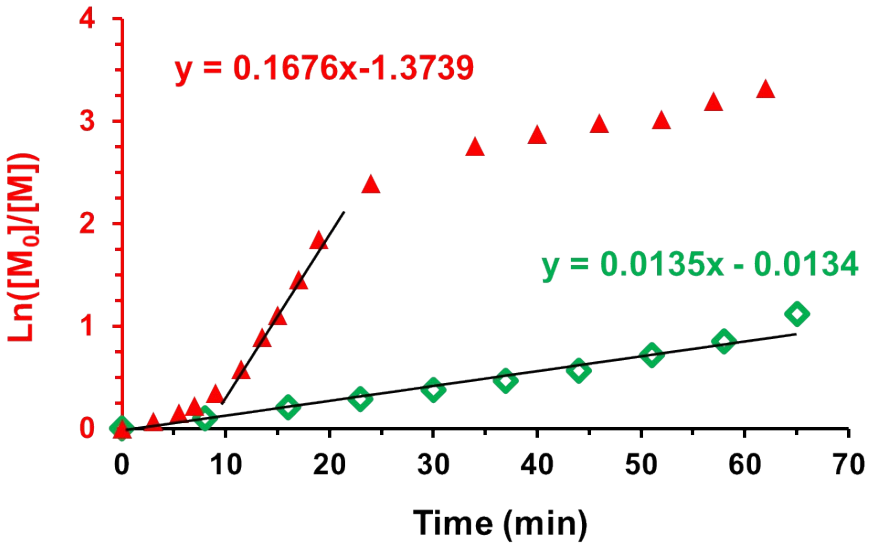

Figure S2. Semilogarithmic plots obtained for the RAFT dispersion homopolymerization of either HPMA or BzMA in mineral oil at 90 °C targeting either 15% w/w $PSMA_9$-$PHPMA_{150}$ vesicles (red triangles) or 18% w/w $PSMA_9$-$PBzMA_{150}$ vesicles (open green diamonds).

Table S1. Summary of the GPC, DLS and TEM data obtained for a series of $PSMA_9$-$PHPMA_x$ diblock copolymer nano-objects prepared at 15% w/w in mineral oil. The $PSMA_9$ precursor is also included as a reference.

Target Composition	Solids Content (% w/w)	THF GPC		DLS		TEM Morphology
		M_n (g mol^{-1})	M_w/M_n	D (nm)	PDI	
$PSMA_9$ macro-CTA	-	4,500	1.12	-	-	-
$PSMA_9$-$PHPMA_{30}$	15	8,100	1.16	23	0.20	Spheres
$PSMA_9$-$PHPMA_{50}$	15	10,000	1.16	26	0.09	Spheres
$PSMA_9$-$PHPMA_{60}$	15	11,000	1.16	34	0.18	Spheres
$PSMA_9$-$PHPMA_{70}$	15	11,900	1.19	40	0.12	Spheres
$PSMA_9$-$PHPMA_{80}$	15	12,800	1.19	57	0.12	Mixed
$PSMA_9$-$PHPMA_{90}$	15	13,600	1.22	104	0.11	Mixed
$PSMA_9$-$PHPMA_{100}$	15	14,400	1.25	153	0.25	Mixed
$PSMA_9$-$PHPMA_{105}$	15	14,300	1.22	170	0.16	Mixed
$PSMA_9$-$PHPMA_{110}$	15	14,700	1.24	204	0.28	Mixed
$PSMA_9$-$PHPMA_{115}$	15	15,000	1.26	156	0.11	Mixed
$PSMA_9$-$PHPMA_{125}$	15	16,400	1.26	156	0.05	Mixed
$PSMA_9$-$PHPMA_{130}$	15	17,000	1.29	162	0.03	Vesicles
$PSMA_9$-$PHPMA_{150}$	15	18,800	1.37	170	0.07	Vesicles

Table S2. Summary of the GPC, DLS and TEM data obtained for a series of $PSMA_9$-$PHPMA_x$ diblock copolymer nano-objects prepared at 20% w/w in mineral oil.

Target Composition	Solids Content (% w/w)	THF GPC		DLS		TEM Morphology
		M_n (g mol^{-1})	M_w/M_n	D (nm)	PDI	
$PSMA_9$-$PHPMA_{30}$	20	7,700	1.15	19	0.12	Spheres
$PSMA_9$-$PHPMA_{50}$	20	10,100	1.16	27	0.10	Spheres
$PSMA_9$-$PHPMA_{55}$	20	10,500	1.18	30	0.12	Spheres
$PSMA_9$-$PHPMA_{60}$	20	12,000	1.24	34	0.12	Spheres
$PSMA_9$-$PHPMA_{65}$	20	11,500	1.19	53	0.14	Mixed
$PSMA_9$-$PHPMA_{70}$	20	12,400	1.31	76	0.16	Mixed
$PSMA_9$-$PHPMA_{75}$	20	12,300	1.20	87	0.16	Mixed
$PSMA_9$-$PHPMA_{80}$	20	13,600	1.30	148	0.22	Mixed
$PSMA_9$-$PHPMA_{90}$	20	14,400	1.34	420	0.73	Mixed
$PSMA_9$-$PHPMA_{100}$	20	14,200	1.23	162	0.17	Mixed
$PSMA_9$-$PHPMA_{105}$	20	14,300	1.24	176	0.13	Mixed
$PSMA_9$-$PHPMA_{110}$	20	15,700	1.25	177	0.14	Mixed
$PSMA_9$-$PHPMA_{115}$	20	16,300	1.26	169	0.11	Vesicles
$PSMA_9$-$PHPMA_{120}$	20	16,700	1.27	182	0.14	Vesicles
$PSMA_9$-$PHPMA_{125}$	20	17,100	1.32	233	0.22	Vesicles
$PSMA_9$-$PHPMA_{130}$	20	17,600	1.28	211	0.14	Vesicles
$PSMA_9$-$PHPMA_{150}$	20	20,100	1.37	573	0.11	Vesicles

Table S3. Summary of the GPC, DLS and TEM data obtained for a series of $PSMA_9$-$PHPMA_x$ diblock copolymer nano-objects prepared at 25% w/w in mineral oil.

Target Composition	Solids Content (% w/w)	THF GPC		DLS		TEM Morphology
		M_n (g mol^{-1})	M_w/M_n	D (nm)	PDI	
$PSMA_9$-$PHPMA_{50}$	25	9,900	1.15	31	0.19	Spheres
$PSMA_9$-$PHPMA_{60}$	25	11,000	1.17	85	0.42	Mixed
$PSMA_9$-$PHPMA_{70}$	25	12,600	1.19	156	0.54	Worms
$PSMA_9$-$PHPMA_{80}$	25	12,700	1.19	1715	0.80	Mixed
$PSMA_9$-$PHPMA_{85}$	25	13,000	1.22	437	0.75	Mixed
$PSMA_9$-$PHPMA_{90}$	25	13,300	1.21	276	0.40	Mixed
$PSMA_9$-$PHPMA_{100}$	25	14,700	1.23	256	0.35	Mixed
$PSMA_9$-$PHPMA_{105}$	25	15,000	1.24	210	0.16	Mixed
$PSMA_9$-$PHPMA_{110}$	25	15,700	1.24	189	0.16	Mixed
$PSMA_9$-$PHPMA_{115}$	25	16,000	1.25	318	0.35	Vesicles
$PSMA_9$-$PHPMA_{120}$	25	16,000	1.25	246	0.24	Vesicles
$PSMA_9$-$PHPMA_{125}$	25	17,200	1.26	445	0.19	Vesicles
$PSMA_9$-$PHPMA_{150}$	25	18,700	1.28	448	0.27	Vesicles

Table S4. Summary of the GPC, DLS and TEM data obtained for a series of $PSMA_9$-$PHPMA_x$ diblock copolymer nano-objects prepared at 30% w/w in mineral oil.

Target Composition	Solids Content (% w/w)	THF GPC		DLS		TEM Morphology
		M_n (g mol^{-1})	M_w/M_n	D (nm)	PDI	
$PSMA_9$-$PHPMA_{40}$	30	9,000	1.15	22	0.15	Spheres
$PSMA_9$-$PHPMA_{50}$	30	9,900	1.16	26	0.07	Mixed
$PSMA_9$-$PHPMA_{60}$	30	10,200	1.16	46	0.12	Mixed
$PSMA_9$-$PHPMA_{67}$	30	11,400	1.18	157	0.58	Worms
$PSMA_9$-$PHPMA_{70}$	30	12,100	1.21	736	0.91	Worms
$PSMA_9$-$PHPMA_{80}$	30	12,300	1.22	471	0.60	Mixed
$PSMA_9$-$PHPMA_{90}$	30	14,300	1.24	715	0.66	Mixed
$PSMA_9$-$PHPMA_{100}$	30	15,000	1.27	923	1.00	Mixed
$PSMA_9$-$PHPMA_{110}$	30	16,000	1.26	219	0.21	Mixed
$PSMA_9$-$PHPMA_{120}$	30	16,900	1.31	1400	0.97	Mixed
$PSMA_9$-$PHPMA_{130}$	30	17,800	1.35	764	0.26	Mixed

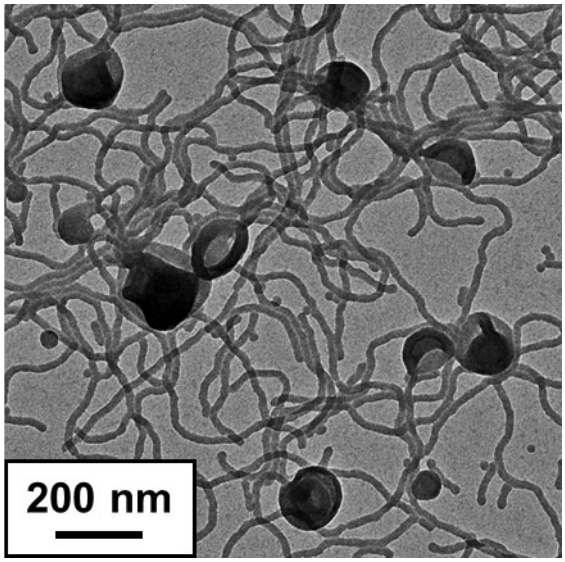

Figure S3. Representative TEM image recorded for a mixed phase of $PSMA_9$–$PHPMA_{70}$ vesicles and worms (prepared at 25% w/w solids) obtained after oscillatory rheology studies.

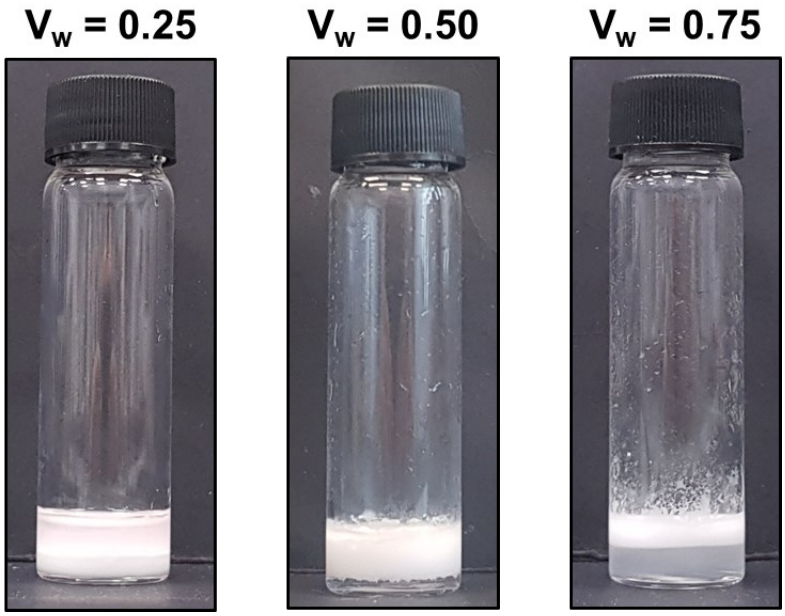

Figure S4. Digital photographs obtained for the Pickering emulsions prepared at 20 °C *via* high-shear homogenization at 13 500 rpm for 2 min using 1.0% w/w $PSMA_9$–$PHPMA_{50}$ spheres in mineral oil at water volume fractions (V_w) of 0.25, 0.50 or 0.75. Sedimentation of the denser aqueous droplets occurs for the emulsion prepared at a water volume fraction of 0.25, indicating the formation of a water-in-oil emulsion. In contrast, preparing the emulsions at a water volume fraction of 0.50 or 0.75 leads to droplet creaming, indicating the formation of (mainly) oil droplets within an aqueous continuous phase.

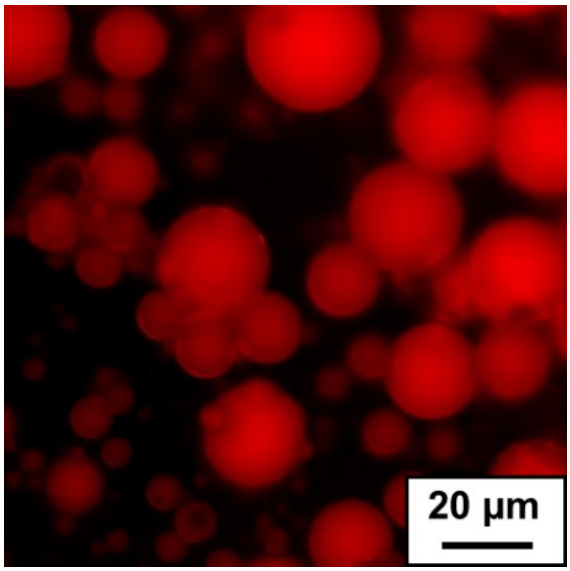

Figure S5. Fluorescence microscopy image recorded for an emulsion prepared using 1.00% w/w $PSMA_9$-$PHPMA_{50}$ diblock copolymer spheres in mineral oil at a water volume fraction of 0.875. The location of the oil-soluble Nile Red dye suggests the formation of a (mainly) oil-in-water emulsion. However, some of the droplets contain dark domains, indicating the formation of a water-in-oil-in-water double emulsion.

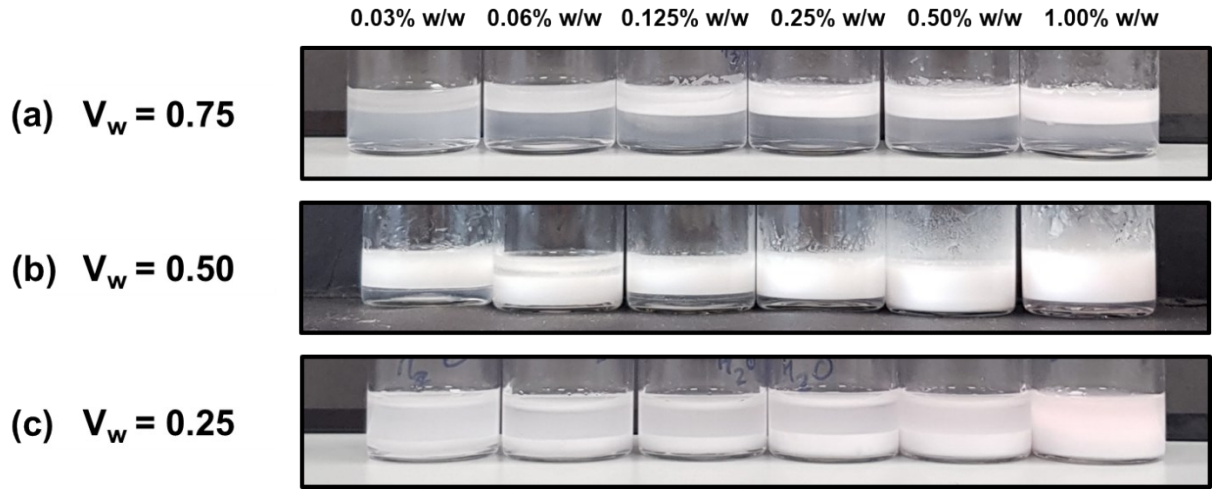

Figure S6. Digital photographs recorded for a series of Pickering emulsions prepared at 20 °C *via* high-shear homogenization at 13 500 rpm for 2 min using 0.03 to 1.00% w/w $PSMA_9$–$PHPMA_{50}$ spheres at water volume fractions (V_w) of (a) 0.75, (b) 0.50 or (c) 0.25.

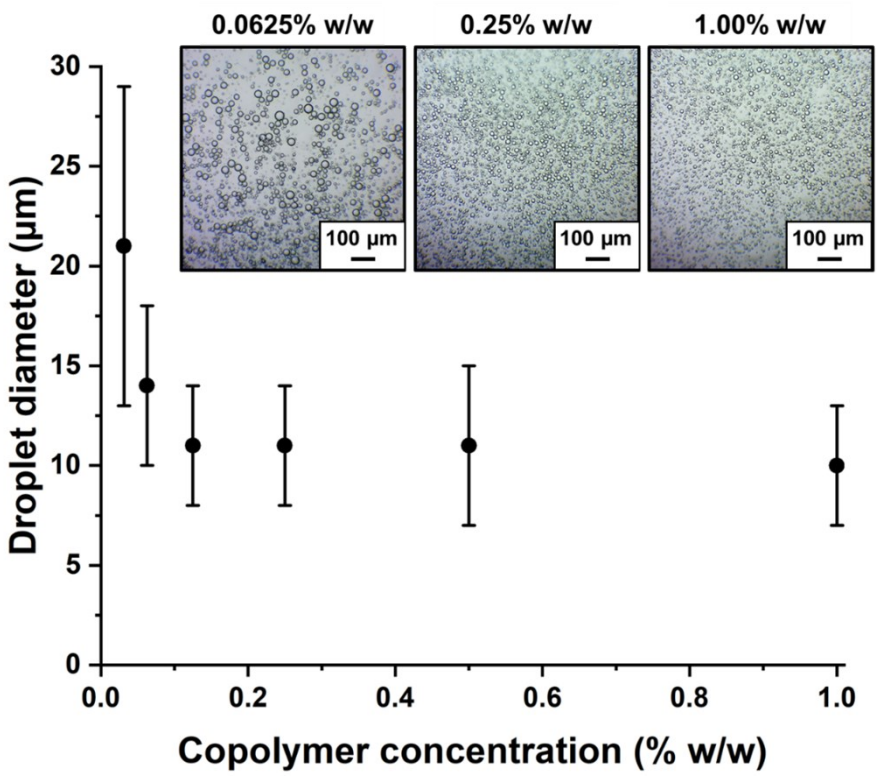

Figure S7. Variation in number-average droplet diameter (estimated from optical microscopy images by analyzing at least 100 droplets in each case) with copolymer concentration obtained for water-in-oil Pickering emulsions produced *via* high-shear homogenization (13 500 rpm for 2 min at 20 °C) of $PSMA_9$-$PHPMA_{50}$ diblock copolymer spheres in mineral oil at a constant water volume fraction of 0.25. Inset: representative optical microscopy images recorded for aqueous droplets prepared using copolymer concentrations of 0.0625, 0.25 or 1.00% w/w, respectively.

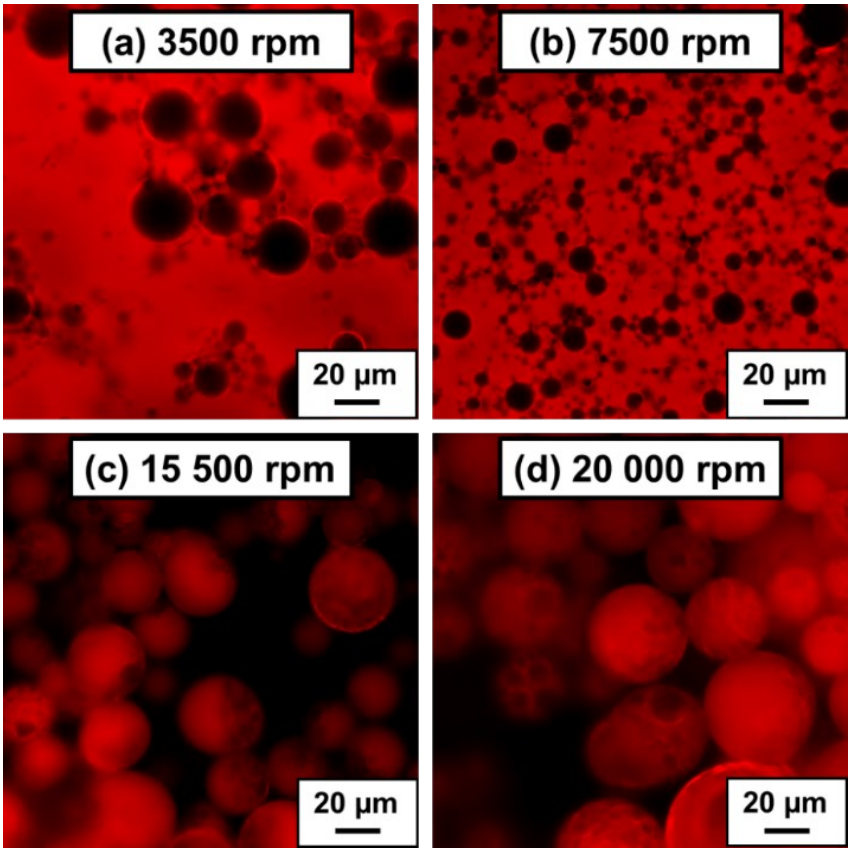

Figure S8. Fluorescence microscopy images recorded for the emulsions formed *via* high-shear homogenization at the stated stirring rate using 1.00% w/w $PSMA_9$-$PHPMA_{50}$ diblock copolymer spheres in mineral oil and a constant water volume fraction of 0.50. Lower stirring rates (either 3 500 or 7 500 rpm) lead to the formation water-in-oil emulsions, whereas higher stirring rates (15 500 or 20 000 rpm) generate water-in-oil-in-water double emulsions.